Pure Appl. Geophys.

https://doi.org/10.1007/s00024-023-03331-w

Pure and Applied Geophysics

Observing the Agulhas Leakage Source in the Water Mixing Area

T. V. Belonenko,[1] M. V. Budyansky,[2] A. A. Malysheva,[1] and A. A. Udalov[2]

Abstract—In this paper, we study the region of the Agulhas leakage origin. The study region is limited by 20–46° S, 0–24° E; it includes the Cape Basin and is crossed by Walvis Ridge. This region is characterized by high dynamic activity of mesoscale eddies and variability of hydrographic parameters in a wide range of spatial and temporal scales. The main element of large-scale circulation is represented by a phenomenon called the Agulhas leakage which is influenced by the South Atlantic Gyre, Benguela Current, and Benguela upwelling. Water particles of various origins are mixed and affect the thermohaline properties of mesoscale eddies, which form a source of the Agulhas leakage. We divided the region into three zones and showed that eddies and their properties differ in each of them. The Agulhas leakage is formed only by long-lived eddies, mainly anticyclones, while cyclones have smaller trajectories and shorter lifespans. In this research, we apply statistical analysis using AMEDA (Angular Momentum Eddy Detection Algorithm), Lagrangian analysis, and the study of vertical thermohaline cross-sections. We establish that in the Cape Basin, the waters of the Agulhas leakage mix with waters of the South Atlantic Gyre and the Benguela Current, and the thermohaline properties of the Agulhas eddies change since the warm and salty waters of the Indian Ocean mix with fresher and colder ones of the Atlantic Ocean. The water particles of the South Atlantic Gyre cross the western border of the region and travel a distance exceeding 500 km in the eastern direction mixing with other particles. We demonstrate that the eddies generated in the Cape Basin are also significantly influenced by the waters of the South Atlantic Gyre. These waters are transported to the Cape Basin region from the west and southwest. This explains the existence of a two-mode water structure noted by other researchers.

Keywords: Agulhas leakage, Cape basin, Agulhas current, South Atlantic Gyre, Benguela current, AMEDA, Lagrangian analysis.

1. Introduction

The study of mesoscale eddies provides an idea of whole systems of interrelated oceanic characteristics. Dynamics of mesoscale eddies is dominated by nonlinear effects. Unlike waves, mesoscale eddies can transfer heat, mass, kinetic energy, and biochemical characteristics from the region of their formation over vast distances, affecting climate fluctuations (Gordon et al, 1992a, 1992b; Donners et al, 2004; Biastoch et al., 2008; Belonenko et al., 2020; Prants, 2020; Malysheva et al., 2020; Budyansky, 2022). Mesoscale eddies are formed almost everywhere in the World Ocean (Chelton et al., 2011), however, the region of eddy activity are generally confined to the regions of large-scale flows, due to the presence of baroclinic and barotropic instability of these flows. They arise due to the vertical and horizontal velocity shears, as well as due to the heterogeneous distribution of water density, which is one of the main conditions for the generation of mesoscale eddies (Pedlosky, 1987). The region located to the southwest of Africa is one of the most dynamically complex basins of the World Ocean and is characterized by the greatest variability of oceanographic fields in the entire range of spatial and temporal scales (Lutjeharms & Ballegooyen, 1988). Here mesoscale eddies can both originate and drift, interacting with the Agulhas current. According to a study by Olson and Evans (1986a, 1986b), the rings of the Agulhas Current are on average 240 ± 40 km in diameter, the orbital rotation speed varies between 30 cm/s and 90 cm/s, and the speed of motion is from 5.5 cm/s to 9 cm/s (from 5 to 8 km/day). However, recent studies have shown that the rates of drift of the Agulhas Current rings can vary in a much wider range (Byrne et al., 1995; Gnevyshev et al., 2021; Schouten et al., 2000).

Supplementary Information The online version contains supplementary material available at https://doi.org/10.1007/s00024-023-03331-w.

[1] St. Petersburg State University, 7–9, Universitetskaya Nab., St. Petersburg 199034, Russia. E-mail: btvlisab@yandex.ru

[2] Pacific Oceanological Institute of the Russian Academy of Sciences, 43 Baltiiskaya St., Vladivostok 690041, Russia.

Published online: 30 July 2023

The Agulhas Current is the main source of warm and salty water transported from the Indian Ocean to the Atlantic. In the study region south of the African coast (Fig. 1), the Agulhas Current makes a sharp turn to the east, forming a loop with a diameter of 340 km. This phenomenon is called the Agulhas Retroflection (Lutjeharms & Ballegooyen, 1988; Lutjeharms & Valentine, 1988). The Agulhas Retroflection periodically forms separate anticyclonic rings consisting of warm and salty waters of the Indian Ocean. The temperature in the rings is 5° C higher and salinity is 0.3 psu higher than the temperature and salinity of the surrounding waters of equal density (Gordon, 1985). Moving at an average speed of 12 cm/s, the rings quickly disintegrate, forming eddies of smaller scales (mesoscale eddies), which retain their characteristic properties, at least up to 5 °E in the western direction and up to 46° S in the southern direction (Lutjeharms & Ballegooyen, 1988; Malysheva et al., 2018, 2020; Sandalyuk & Belonenko, 2018). At least four to six rings of the Agulhas Current appear in the Cape Basin every year and are responsible for a mass transport of 2.6–3.8 Sv between the two basins (Duncombe Rae et al., 1996; Garzoli & Gordon, 1996). The decay of the Agulhas rings with the subsequent formation of smaller-scale eddies has been well studied in the models (Kamenkovich et al., 1996; Drijfhout & de Vries, 2003; Donners et al., 2004; De Steur et al., 2004; Doglioli et al., 2007; De Steur), as well as in the field studies (Byrne et al., 1995; Goni et al., 1997; Olson & Evans, 1986a, 1986b; Schmid et al., 2003; Schouten et al., 2000). These eddies can travel over hundreds (and even thousands) of kilometers, which indicates great potential for exchange. That is why they can be studied as special natural tracers of water exchange between the Indian and Atlantic oceans and have a significant impact on the climate (Donners et al, 2004; Gordon et al, 1992a, 1992b). This phenomenon is called the Agulhas leakage. It refers to the waters exported to the Atlantic Ocean by the Agulhas current system. These waters consist mainly of upper and intermediate waters of the Indian Ocean (Doglioli et al, 2006).

The effect of the Agulhas leakage on the general circulation in the Atlantic Ocean occurs in two modes: through the radiation of planetary waves and advection. The warm and saltier waters of the Indian Ocean (compared to the surrounding Atlantic waters, which leads to inclined isotherms and isohalines in the thermocline) flowing into the Cape Agulhas region generate disturbances in the form of slowly propagating Rossby waves in the South Atlantic and isopycnic inhomogeneities. Thus, a system of coherent eddies moving westward is formed (Biastoch et al., 2008; Malysheva et al., 2018, 2020). Agulhas eddies formed by the barotropic and

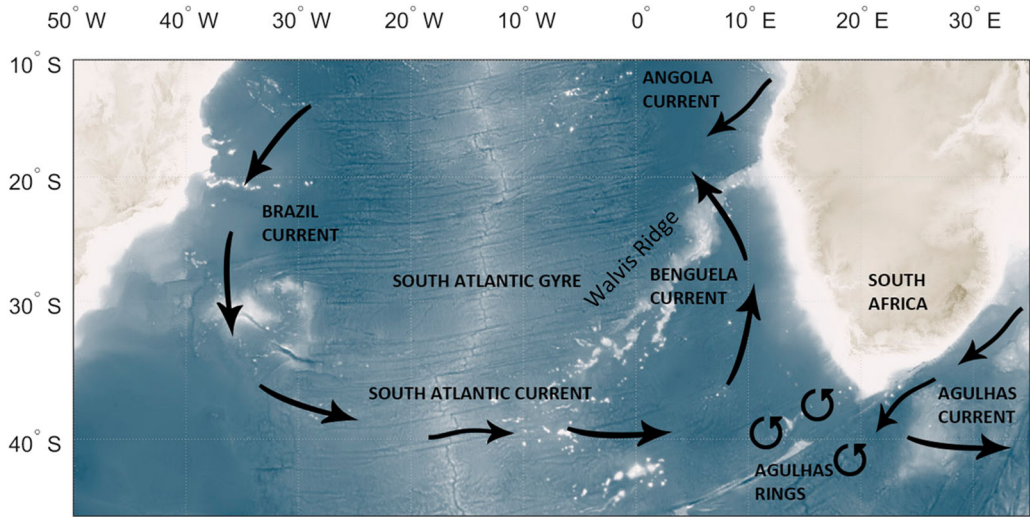

Figure 1
General circulation scheme of the area under consideration

baroclinic instability of the Agulhas Current cross the South Atlantic (see pls Fig. 2), feeding the surface waters of the Atlantic meridional overturning circulation with warm and salty waters of the Indian Ocean (Gordon & Haxby, 1990; Malysheva et al., 2018, 2020). These eddies were studied using satellite images of sea surface temperature and altimeter data (Byrne et al., 1995, Beismann et al., 1999, Schouten et al, 2000, Doglioli et al., 2007). In the literature, quantitative estimates of the Agulhas leakage range: from 4 Sv (1 Sv = 10^6 m^3 s^{-1}) (Schmitz, 1995) to 22 Sv (Donners et al, 2004). However, most studies based on different methods report values of 11–17 Sv (Gordon et al., 1987; Gordon & Haxby, 1990; Gordon et al., 1992a, 1992b; De Ruijter et al., 2002; Reason et al., 2003; Bryden et al., 2005; Richardson, 2007; Cheng et al., 2016; Durgadoo et al., 2017; Van Sebille et al., 2009; Malysheva et al., 2020).

However, Wang et al. (2015) using the accurate technique of frame-independent identification of mesoscale eddies with cores whose material boundaries remain coherent, i.e., without showing noticeable signs of filamentation derived the coherent transport computation, which turned out to be smaller (by at least 2 orders of magnitude) than earlier ring transport estimates, for up to 1 year. Nonzero transport estimates range approximately from 0.25 to 3 Sv (about 1.5 Sv on average). The authors do not believe in the correctness of the conceptual pattern, in which Agulhas rings are shed from the Agulhas retroflection as a result of episodic Indian-Ocean-water-entrapping occlusions. Coherent material eddies tend to emerge near the Walvis Ridge from rather incoherent flows of water, mostly residing in the South Atlantic and to a small extent traceable into the Indian Ocean. How this precisely happens is not known and is the subject of an ongoing investigation. Moreover, they indicate that only one eddy consisting of mainly Indian Ocean water was seen to transport its contents to the North Brazil Current. This suggests that the contribution of coherent material Agulhas rings to the global thermodynamical budget is much less significant than originally thought (Gordon & Haxby, 1990). Malysheva et al. (2020) confirm that only one long-lived eddy reached the flow of the North Brazil Current. Note that very few mesoscale eddies cross the Mid-Atlantic Ridge (Gnevyshev et al., 2021; see pls Fig. 2 in Malysheva et al., 2020).

Note that in the Cape Basin, where eddies are generated as a result of the destruction of the Agulhas rings, the Agulhas waters mix with the waters of the South Atlantic Gyre and Benguela Current extending north along the western coast of South Africa (Hutchings et al., 2009). Although there is no

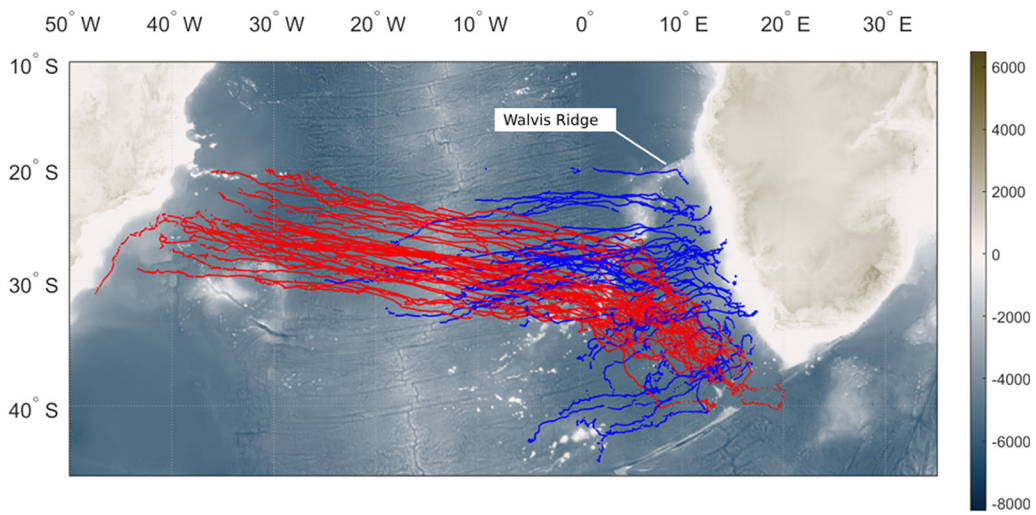

Figure 2
Tracks of 40 long-lived individual anticyclones (red) and 40 long-lived cyclones (blue) identified by META3.2 for 1993–2021 The color scale shows the depth (m)

consensus on the exact contribution of the Agulhas waters to the Benguela Current, there is a correlation between the strength of the Benguela Current and the eddy transport of the Agulhas Current (Garzoli & Gordon, 1996). Moreover, Matano & Beier (2003) found that most of the energy of the Benguela Current is provided by the Agulhas eddies, i.e. the Benguela current can be considered as a means of facilitating the transport of the Agulhas eddies to the Atlantic Ocean. But it cannot be denied that the structure of eddies generated in the Cape Basin is also significantly influenced by the waters of the South Atlantic Gyre (Fig. 1). These are the waters that arrive to the Cape Basin region from the west and southwest.

The destruction of large Agulhas rings with a diameter of 300–400 km leads to the formation of numerous eddies (Duncombe Rae, 1991; Gordon & Haxby, 1990; Lutjeharms & van Ballegooyen, 1988; Olson & Evans, 1986a, 1986b). These eddies are mainly anticyclonic, have a diameter of 100–200 km, and the lifespan often exceeds 1 year. They are the main component of the Agulhas leakage (Garzoli & Gordon, 1996; Gordon et al., 1992a, 1992b; Sandalyuk & Belonenko, 2018). On the contrary, mesoscale eddies formed directly in the Benguela current, mainly cyclonic, have a diameter of about 100 km (Sandalyuk & Belonenko, 2018).

Thus, there is a basin off the southwestern coast of South Africa where the Agulhas eddies interact with the waters of the South Atlantic Gyre and the Benguela Current. Guerra et al. (2022) considered temperature and salinity profiles from 1993 to 2016, and they analyzed more than 3200 temperature profiles and 2400 salinity profiles from historical databases and compared them with 52 long-lived Agulhas eddies. This analysis revealed that in 88% of cases, all profiles can be attributed to two types of water: type I, temperature $16.2 \pm 0.6°$ C, salinity 35.6 ± 0.1, and type II, temperature $12.9 \pm 0.7°$ C, salinity 35.2 ± 0.1. We believe that the first type of water is formed by the warm and salty waters of the Agulhas Current, which carries the properties of the Indian Ocean, while the second type is formed by the cold and fresher waters of the South Atlantic Gyre and the Benguela Current. However, both types of water were simultaneously detected inside the majority of eddies formed in the Cape Basin (67%) (Guerra et al., 2022).

Thus, not only the Agulhas Current eddies but also the eddies directly formed in the Cape Basin, transport the waters of the Agulhas leakage to the Atlantic (Fig. 2). They play an important role in the interoceanic transfer of heat, salt, and mass. The interaction of the Agulhas eddies with the waters of the South Atlantic Gyre and the Benguela Current is a unique process and is not found in any other major system of the eastern boundary currents.

However, the role of the South Atlantic Gyre and the Benguela Current in the Agulhas leakage and the spatial distribution of water particles of different origins in the interaction zone of the Cape Basin has not been analyzed by anyone before. This paper is an attempt to eliminate the existing gap. Thus, the goal of our study is to analyze the spatial distribution of water particles of various origins in the region of eddy generation in the Cape Basin. For the study, we use statistical analysis using AMEDA (Sect. 3.2), the Lagrangian modeling method (Sect. 3.3), and thermohaline analysis of water (Sect. 3.4).

2. *Data and Methods*

We used GLORYS12V1 (Global Ocean Physics Reanalysis) data available on the CMEMS portal (Copernicus Marine Environment Monitoring Service). GLORYS12V1 is an eddy-resolving reanalysis of the World Ocean with a spatial resolution of 1/12° and 50 vertical levels for a period where altimetric observations are available. It is based on the CMEMS global real-time prediction system. The NEMO model with the ECMWF ERA-Interim forcing is used for simulating oceanic conditions. The data of observations are assimilated with the help of a low-order Kalman filter. Data from satellite altimeters (sea level anomaly), sea surface temperature, sea ice concentration, and vertical profiles of the temperature and salinity are assimilated together in situ. This product includes daily 3D fields of the potential temperature, salinity, and currents, as well as 2D fields of sea surface height, depth of the upper quasi-uniform layer, bottom potential temperature, ice thickness, ice types, and ice drift velocities.

Assimilated observations are Reynolds 0.25° AVHRR-only SST, sea level anomalies from all altimeters, temperature, and salinity profiles from the CMEMS CORAv4.1 database, and ice data from the CERSAT Sea Ice concentration database. The boundary conditions for the temperature and salinity for 1991 were taken according to EN4.0.2 (http://hadobs.metoffice.com/en4/download-en4-0-2.html).

We used "The altimetric Mesoscale Eddy Trajectory Atlas product (META3.2 DT allsat)". It was produced by SSALTO/DUACS and distributed by AVISO + (https://www.aviso.altimetry.fr) with support from CNES, in collaboration with IMEDEA. The product is based on altimetric information (sea surface height) to identify and determine the trajectories of cyclones and anticyclones in the World Ocean (Pegliasco et al., 2022).

The algorithm identifies isolated eddy structures on daily maps and then monitors them, recording their evolution over time. The algorithm identifies eddies as clusters of pixels (maximum size 2000 pixels) that satisfy a certain set of criteria, such as compactness, the presence of an extremum of sea level anomalies inside the eddy, etc. The Atlas gives each eddy its identification number and coordinates of its trajectory. The META3.2 product contains information about the type of eddies, their radius and amplitude, orbital speed, and lifetime.

We used an optimized algorithm AMEDA (Angular Momentum Eddy Detection and Tracking Algorithm) for detecting and tracking eddies from two-dimensional velocity fields. This eddy identification uses a hybrid method based on physical parameters and is applied to the data of the GLORYS12V1 reanalysis. The main advantages of AMEDA are as follows: the algorithm is robust to the grid resolution, it uses a minimal number of tunable parameters, the dynamical features of the detected eddies are quantified, and the tracking procedure identifies the merging and splitting events. The proposed method provides a complete dynamical evolution of the detected eddies during their lifetime. This allows for identifying precisely the formation areas of long-lived eddies, the region where eddy splitting or merging occurs frequently, and eddies interact with the currents (Le Vu et al., 2018). The average orbital speed throughout the circulation along the closed contour (flow) is determined for each contour using the mean radius, which is equivalent to the radius of a circle with the same area. The contour with the maximum orbital speed determines the size of the eddy. Using the AMEDA algorithm, we made the identification of the eddies inferred from the GLORYS12V1 data.

Simulation of water circulation in oceanic basins has been performed within the natural framework using Lagrangian methods, which describe the transport and mixing in a study region computing trajectories of a large number of artificial passive particles. In a turbulent or chaotic flow, plotting trajectories of an ensemble of particles, advected by the satellite-derived or a numerical-model velocity field, results in a tangle of convoluted lines that is difficult to interpret. Based on statistical quantities over ensembles of trajectories, we propose to use specific trajectory functions, Lagrangian indicators, in order to extract information about the circulation from the entangled trajectories and to provide an accurate description of the transport and mixing processes.

The Lagrangian indicators are computed by numerically forming a dense mesh of a large number of artificial particles backward in time starting from a fixed date. Different kinds of indicators can be constructed depending on the task of the research. The outputs depend strongly on the time interval over which trajectories are computed. The longer the integration time, the more information on a simulated trajectory one gets, but, on the other side, the more information is lost when computing an indicator based on this trajectory. It is important to choose an adequate time interval considering the peculiarities of the oceanographic situation in the study region.

The field of a Lagrangian indicator is represented on a basin Lagrangian map for each day. The set of consecutive maps allows one to track the evolution of this field day by day. These maps often resemble patterns with patches, tendrils, and filaments with increased gradients of the indicator values. The lines with prominent horizontal gradients are Lagrangian fronts (Prants et al., 2014, 2017) separating water masses with a distinct history that often coincide with confluence lines and vortex boundaries. The reverse-time analysis of the simulation results allows one to determine where fluid particles passing some point

have arrived from. In the Lagrangian approach, transport processes are tracked by following parcels of water.

which are represented by passive artificial particles. A large number of particles are distributed over the study area. Trajectories of Lagrangian particles are computed by solving the advection equations

$$\frac{d\lambda}{dt} = u(\lambda, \varphi, t), \frac{d\varphi}{dt} = v(\lambda, \varphi, t), \quad (1)$$

where u and v are angular zonal and meridional components of the GLORYS velocity field, and φ and λ are latitude and longitude. The angular velocities are used because the equations for them have a maximally simple form on the Earth's sphere. Bicubic spatial interpolation and smoothing of the temporal evolution by the third-order Lagrangian polynomials are used to provide accurate numerical results. The Lagrangian trajectories are computed by integrating Eqs. (1) using the fourth-order Runge–Kutta scheme with the constant time step of 0.001 days.

For each particle, the length of its trajectory

$$S = R_E \int_{t_1}^{t_2} \sqrt{(\lambda'(t))^2 \cos^2 \varphi(t) + (\varphi'(t))^2}\, dt \quad (2)$$

is calculated for a given period (30 days in the current study). It is just the length of the curve traced by a trajectory of the advected particle from its initial position $(\varphi(t_1),\lambda(t_1))$ to the final one $(\varphi(t_2),\lambda(t_2))$, where $\varphi'(t)$ and $\lambda'(t)$ are the derivatives over time and R_E = 6371 km is the Earth's radius (Budyansky et al., 2022).

To identify the eddy's centers, and track the motion of eddies and their impact on surrounding waters, we compute locations of stationary points with zero velocity in all the model layers and record them every day. The standard stability analysis of the linearized advection equations is then performed to specify the stagnation points of elliptic and hyperbolic type (for details see Prants et al., 2017). The stable elliptic points (triangles on the maps) are located at the centers of eddies where rotation prevails over deformation. The birth of an eddy is manifested by the appearance of an elliptic point, whereas its disappearance signals the decay of the eddy. The hyperbolic points with associated stable and unstable manifolds organize the flow around eddies to cause water exchange with the surrounding waters. The hyperbolic points (orange crosses on the maps), where deformation prevails over rotation, are located mostly between eddies. Any hyperbolic point has directions in which water particles approach it and directions in which they move away. In the theory of dynamical systems, such geometric structures are known as stable (attracting) and unstable (repelling) manifolds.

In this paper, we apply this approach to study and document the transport of water masses in the study region where the Cape Basin is located; hence, we can monitor the evolution of the eddies there. With this aim, we compute various Lagrangian indicators plotting the results on the corresponding Lagrangian maps. To track the origin of water masses and their distribution in the area, we compute the so-called origin maps (O-maps), which show by different colors the regions where the water parcels in the area arrived from (Prants et al., 2018). Integrating advection equations backward in time, we get an O-map where particles are colored following the geographical border that they crossed in the past. The O-maps are also parameterized by the starting day and the integration period which has been found empirically as T = 365 days. To reveal the origin region of fluid particles, present in the study site on a given date, we distribute many particles over the region on this date and compute their trajectories backward in time for 365 days. To calculate each Lagrangian map, an array of particles with initial conditions was selected daily on a uniform grid of 500 × 500 nodes in the specified region 20–46 °S, 0–20 °E. The particles, crossing the northern, southern, eastern, and western borders of the study region during that period, are marked on the O-maps by blue, yellow, red, and green colors, respectively. If a particle remained in the study area for more than 365 days, it is shown by white. We use the GLORYS12V1 data at a depth of 266 m for the Lagrangian analysis. We chose this depth to exclude the effect of Benguela upwelling and eddies generated in the upwelling.

3. Results

3.1. Number of Mesoscale Eddies Based on META3.2

Using META3.2 for the study region (20–46° S, 0–24° E), we detected 54,496 eddies of the Agulhas Current for 1993–2017, of which 28,018 cyclones and 26,478 anticyclones. It turned out that only anticyclones are long-lived eddied of the Agulhas Current with life-times exceeding a year. The tracks of the Agulhas anticyclones with a lifespan > 2.5 years in the South Atlantic are analyzed by Gnevyshev et al. (2021). Tracks of 40 long-lived individual anticyclones and 40 long-lived cyclones identified by the automatic identification method are shown in Fig. 2. It can be seen that the eddies move to the west, but the tracks of anticyclones tend to deviate to the equator while cyclones turn to the south. The physical mechanisms of this phenomenon are discussed by Gnevyshev et al. (2021).

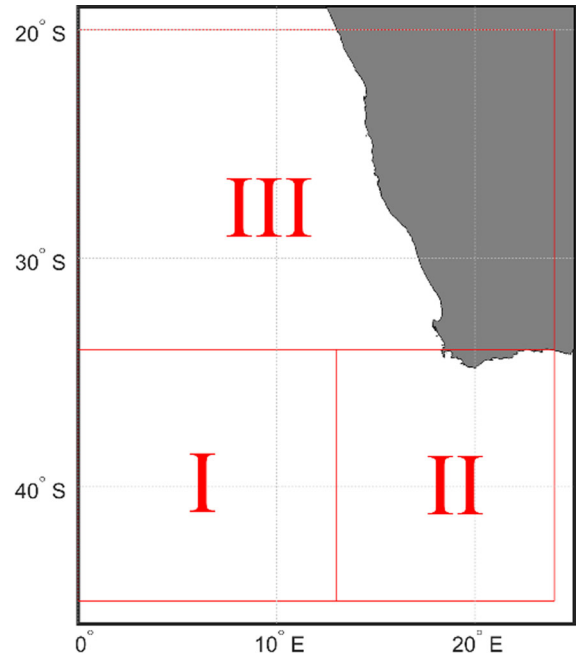

Figure 3
Zones under consideration

3.2. Statistical Analysis of Mesoscale Eddies Based on AMEDA

We divide the region under consideration into three zones: (I)—34–45° S, 0–13° E; (II)—34–45° S, 13–24° E; (III)—20–34° S, 0–24° E (Fig. 3), considering different places of eddy generation and providing the statistical analysis for each individual zone. We consider only long-lived eddies with a lifetime of > 60 days. Note that eddies in three zones differ in the mechanisms of their generation. In Zone I, located in the southwest part of the region, eddies generate due to the barotropic and baroclinic instability of the branches of the South Atlantic Gyre. The places of eddy generation and dissipation are mainly limited to the area boundaries. In Zone II, located in the southeastern part of the region, eddies generate due to the decay and destruction of the Agulhas rings and belong to the Agulhas leakage. The trajectories of these eddies extend to the northwest and are much longer than those of Zone I. Finally, Zone III is located in the northwestern part of the region. The trajectories of the eddies generated there are directed mainly to the west. These eddies have properties of the Indian Ocean waters due to the mixing with waters of the Agulhas leakage. Figure 4 demonstrates the main features of these groups of eddies. Notice that the zonal eddy displacement and, accordingly, the zonal component of the velocity dominate since this is facilitated by the influence of the β-effect. Eddies propagate almost rectilinearly. Under the influence of topography, especially when crossing the Walvis Ridge, the tracks change the propagation azimuth, after which eddies propagate rectilinearly again. We also indicate the tendency of anticyclone tracks to shift to the equator and cyclones to the south. The effect shown in Fig. 1 was reported earlier Gnevyshev et al. (2021).

The numbers of anticyclones (AE) and cyclones (CE) for the period 2009-05-31 to 2020-05-30 in the three zones are shown in Table 1. Then, we provide the statistical analysis for them.

Since AMEDA allows one to detect the eddy centers and their characteristic contours as well as dynamical features associated with the eddies, we can estimate the integral square (km^2) of eddy contours.

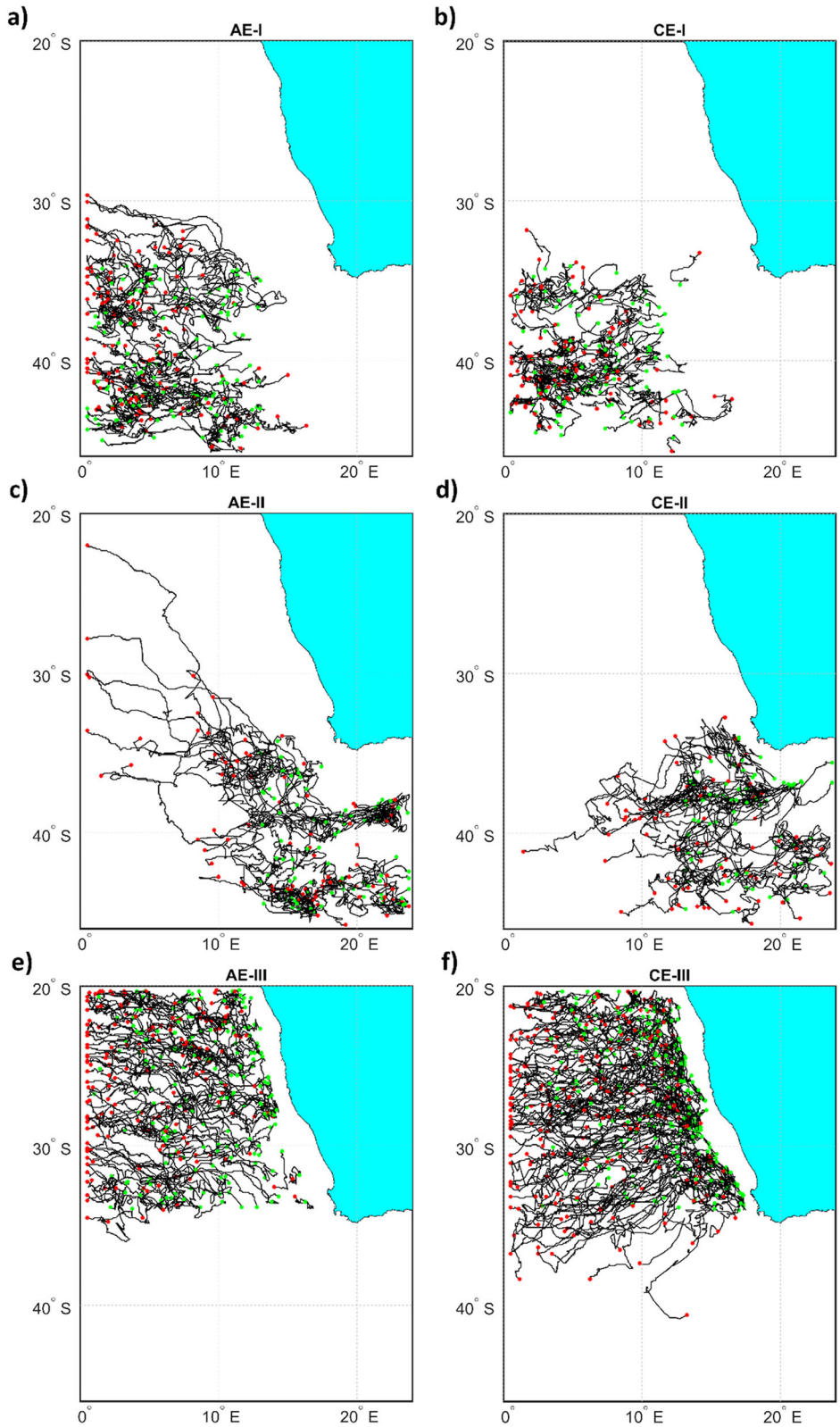
a)
AE-I
b)
CE-I
c)
AE-II
d)
CE-II
e)
AE-III
f)
CE-III
20° S
30° S
40° S
0°
10° E
20° E

◀Figure 4
Trajectories of the individual eddies for Zones I (**a**, **b**), II (**c**, **d**), and III (**e**, **f**). Anticyclones are shown on the left, and cyclones are on the right. The places of generating eddies are shown by green points, and red points indicate the places of eddy dissipation. Only eddies with a lifetime of more than 60 days are considered

Table 1

The numbers (N) of anticyclones (AE) and cyclones (CE) with a lifetime > 60 days in the three zones with area S, and the ratio N of number to area S (see Fig. 3)

Areas (S, km^2) of Zones I-III	N (AE)	N/S (AE) × 10^{-4}	CE	N/S (CE) × 10^{-4}
I (1356 × 10^3)	259	1.91003	267	1.96903
II (1147.3 × 10^3)	159	1.38586	156	1.35971
III (2468.1 × 10^3)	390	1.58016	424	1.71792

Note that Zone III contains the largest number of both individual AE and CE. However, the area of Zone III also exceeds the areas of Zones I and II. The largest number of eddies per unit area is in Zone I where the interaction of the waters of the South Atlantic Gyre with the waters of the Agulhas leakage occurs

Using AMEDA, we provide a distribution of various characteristics for eddies generated in Zones I–III. In Fig. 5 we consider contours for individual eddies with a time step of the data used, i.e., one day of the GLORYS12V1 data. A contour is a daily image of an eddy. If an eddy lives for 100 days, then we have 100 contours, and if 10 eddies with a lifetime of 100 days we have 1000 contours. We estimate an eddy contour area. Figure 5 indicates that the integral area for AEs is much larger than the integral area for CEs despite the number of individual CEs with a lifetime of more than 60 days exceeding the number of long-lived AEs. This illustrates that the number of contours of AEs exceeds significantly the number of contours of CEs, hence, the integral area of AE contours is larger than the integral area of CE contours.

Other characteristics of eddies in Zones I–III are shown in Figures A1–A6 in the Suppl. Mat. The scales (diameters) of AE in Zone I are slightly larger than the ones of CE but in general, the scales are comparable for AE and CE. The radii of most contours of the eddies are 40–50 km (see pls Suppl. Mat., Figure A1). The lifetime distribution of the eddies confirms that AEs are more long-lived than CEs. Note that we considered the lifetime of eddies only within the Zones under consideration. The majority of the eddies located in the Zones have a lifetime less than 100 days. However, some eddies in Zones II and III have a lifetime of more than 500 days (Suppl. Mat., Figure A2). Accordingly, these individual eddies have the longest path length (Suppl. Mat., Figure A3). The mean orbital velocities vary mostly from 0.05 to 0.5 m/s for both AEs and CEs. However, the mean orbital velocities are larger in Zone II where many eddies are generated due to the splitting of the Agulhas rings into some individual eddies (Suppl. Mat., Figure A4). The velocities of drift are of 3–13 km/day (3–15 cm/s) for both AEs and CEs. They are slightly larger for AEs than CEs in all three zones (Suppl. Mat., Figure A5). Finally, the distribution of the non-linearity parameter (the ratio of the orbital speed of the vortex to the speed of its movement) demonstrates significant nonlinearity of the eddies (Suppl. Mat., Figure A6).

3.3. Lagrangian Analysis of Water Particles

Based on the GLORYS12V1 data we provide the Lagrangian analysis of water particles. We consider a region limited by 20–46 °S, 0–20 °E which includes the Cape Basin. We perform an analysis of Lagrangian maps for a depth of 266 m. The choice of this depth makes it possible to exclude the influence of wind and other surface effects, but at the same time, this depth makes it possible to identify the cores of mesoscale eddies located in a layer of 150–800 m (Malysheva et al., 2022; Sandalyuk & Belonenko, 2021). We analyzed 7 types of daily Lagrangian maps for the period May 2010 to April 2020. Further, we consider the main Lagrangian indicators calculated for the region under consideration. Below we present some Lagrangian maps only for certain dates and those for the full period of calculation we demonstrate in Suppl. Mat.

Figure 6 shows the map of particle motion (S-map) for 2013-09-04. The Lagrangian modeling method identifies many cyclones and anticyclones in the region under consideration on the current date. Those eddies that are characterized by large lengths of particle trajectories are highlighted with black color. These particles rotate relative to the centers

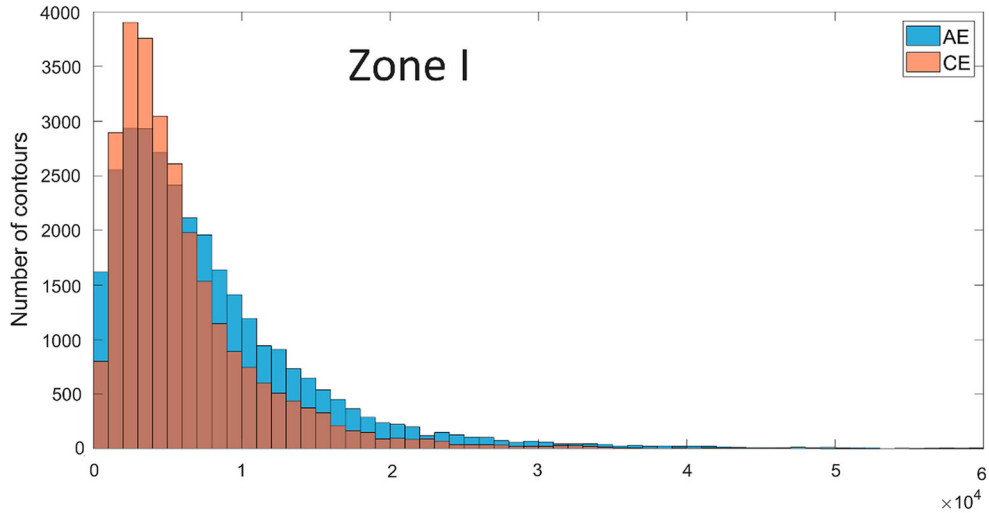
Zone I
AE
CE
Number of contours
4000
3500
3000
2500
2000
1500
1000
500
0
0
1
2
3
4
5
6
×10^4

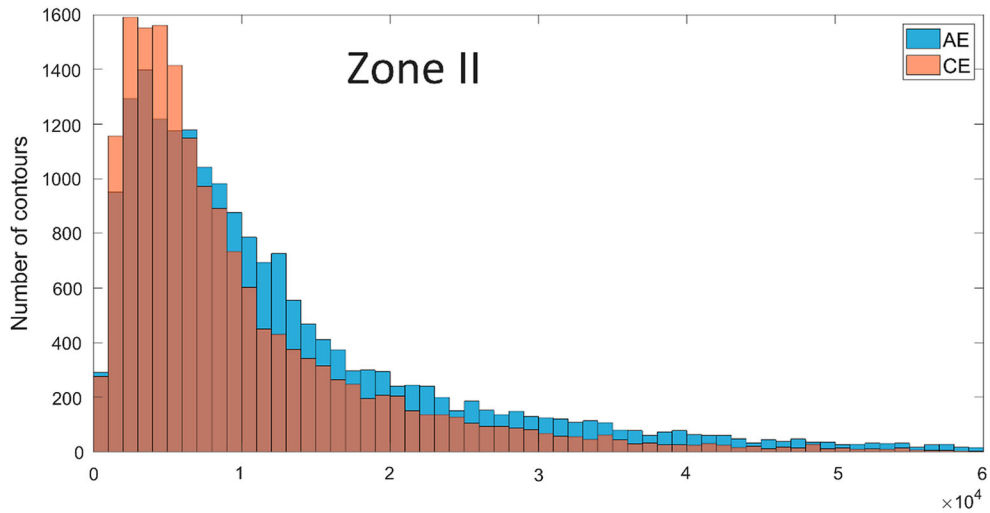
Zone II
AE
CE
Number of contours
1600
1400
1200
1000
800
600
400
200
0
0
1
2
3
4
5
6
×10^4

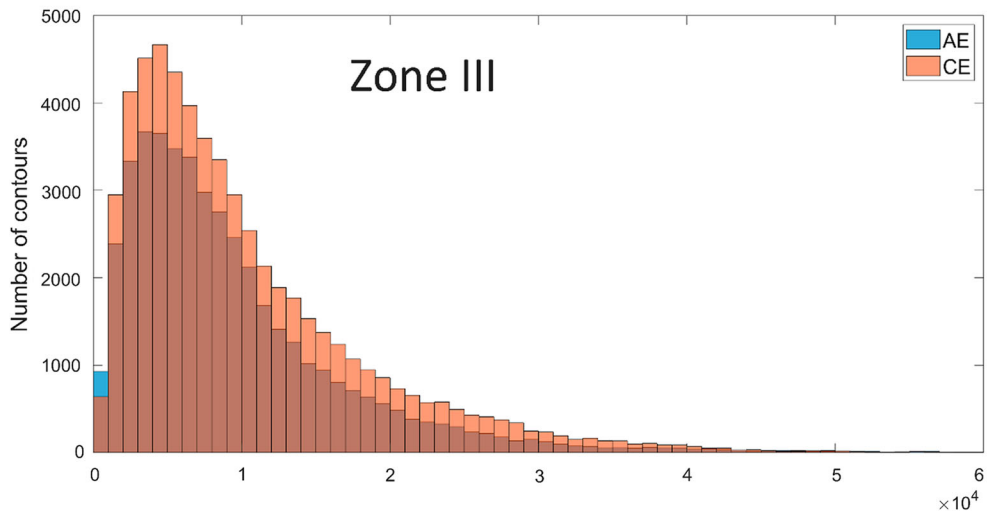
Zone III
AE
CE
Number of contours
5000
4000
3000
2000
1000
0
0
1
2
3
4
5
6
×10^4

◀Figure 5
Distribution of integral area (km^2) of eddy contours for AEs and CEs in Zones I–III. The dark brown color corresponds to the combination of light brown (for CEs) with blue (for AEs)

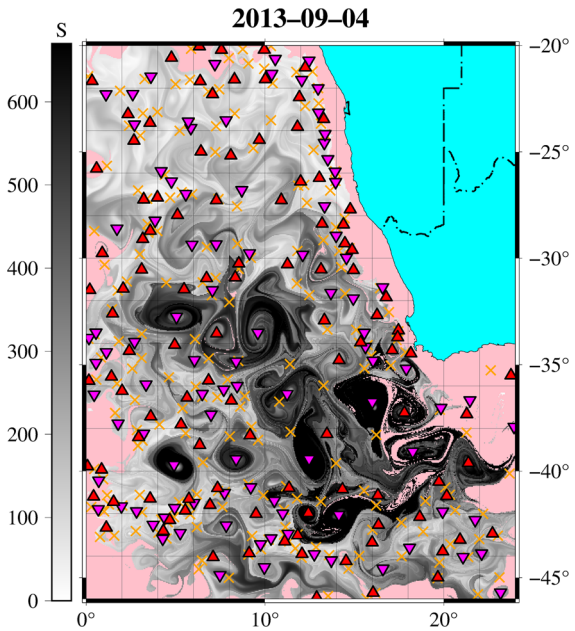

Figure 6
A map of particle motions (Lagrangian S-map) on September 4, 2013, at a depth of 266 m. The black color corresponds to the length of the trajectory that each point (water particle) passed in km 30 days earlier than the date indicated in the title. The pink color corresponds to points belonging to one of two types of waters: the first are those points that touched the mask of the shore (or the contour of the shelf), and the second is those points that in the past reached the edges of the selected box of the velocity field. The triangles represent elliptical points: red triangles represent the centers of cyclones shown filled upward triangle, and crimson triangles represent the centers of anticyclones shown filled downward triangle. The orange crosses show the hyperbolic points which are points of instability

with significant orbital velocities. In other words, a large trajectory length (and the black color of the points) corresponds to the particles that rotate in an eddy or are carried by a jet stream. According to the scale, the maximum saturated black color corresponds to a trajectory length of 700 km. Figure 6 demonstrates a band of eddies, mainly anticyclones that extend from the southern tip of Africa in the direction of the northwest. This phenomenon is a

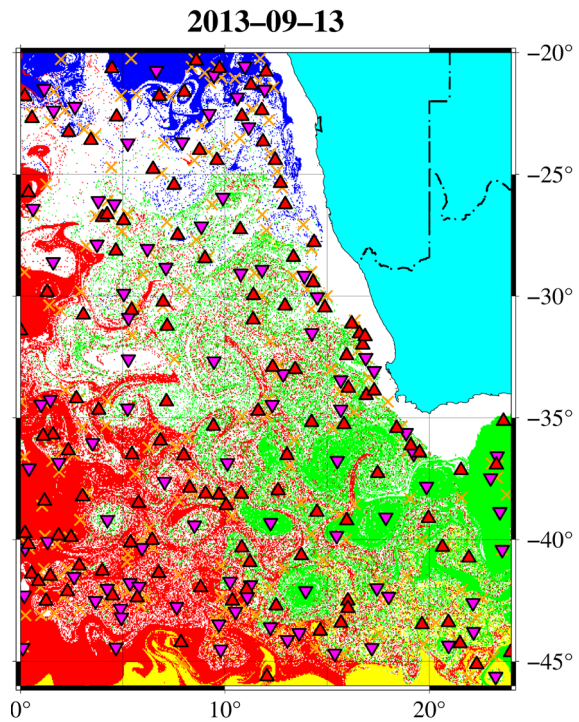

Figure 7
The map of the origin of water masses (Lagrangian O-map) on September 13, 2013, at a depth of 266 m. The points are colored green for the water particles that crossed the meridian 20 °E 365 days ago from this date; yellow is for the particles that crossed 46 °S within a year ago from this date; red is for the particles that crossed the 0° meridian; blue is for the particles that crossed 20 °S. White color is the mask of the shelf from the boundaries of the intersection of the bottom with a depth of 266 m and the coastline on the surface, and also for the particles that have not crossed any of the boxing borders. The triangles represent elliptical points: red triangles represent the centers of cyclones shown filled upward triangle, and crimson triangles represent the centers of anticyclones shown filled downward triangle. The orange crosses show the hyperbolic points which are points of instability

manifestation of the Agulhas leakage on the presented S-map.

Figure 7 shows the origin map (O-map) for the region under consideration. The O-map demonstrates the Lagrangian particles which are distributed at a depth of 266 m. The green color corresponds to the water particles of the Agulhas leakage. This is a band of points on the western side of Africa extended to the northwest. These are the waters of the Agulhas Current that were formed in the Indian Ocean and then crossed 24° E afterward. The yellow color characterizes the particles, that crossed 46° S during the last year. These particles can reveal the southern

part of the South Atlantic Gyre where south-easterly winds cause currents flowing to the east, which is difficult to distinguish from the northern boundary of the Antarctic Circumpolar Current. We can see that the influence of the Antarctic Circumpolar Current is limited to the southern part of the region. The red color characterizes the particles, that crossed the prime meridian during the last year. These water particles arrived from the west and they may originate from the South Atlantic Gyre and affect both the Agulhas leakage and the Benguela Current. The blue color refers to the particles of the Angola Current. Figure 7 shows that the influence of the Angola Current is limited only to the northern part of the region. There are many white points distributed throughout the region in Fig. 7. They correspond to the particles that for 1 year of counting in reverse time could not reach any of their boundaries of the region and coastline.

Figure 8 complements the O-map showing "the age" of the water particles. The T-map shows the period when the particle crosses one of the borders of the area. According to the scale, black color characterizes water particles that crossed the border of the region 1–30 days ago, gray 100–200 days ago, and white 200–365 days ago from the given date. This means that those waters shown in black are "young waters" that recently arrived to the region. On the contrary, the white color indicates the "old waters". One can see that a large number of water particles have not left the region over the past year. Figure 8 shows that "young waters", i.e. particles with a short residence time in the region correspond to the main elements of circulation which are the Agulhas leakage, Antarctic Circumpolar Current, Benguela Current, and Angola Current. At the same time, a large number of particles in the region does not differ in any significant mobility and they are painted white in Fig. 8.

Figures 9 and 10 demonstrate the zonal and meridional displacement of the water particles. These figures show that the main and most important element of circulation in the area under consideration is the Agulhas leakage but it is influenced by the waters that arrived from the west. The particles cross the western border of the study and travel eastward a distance exceeding 2700 km during a year and mix

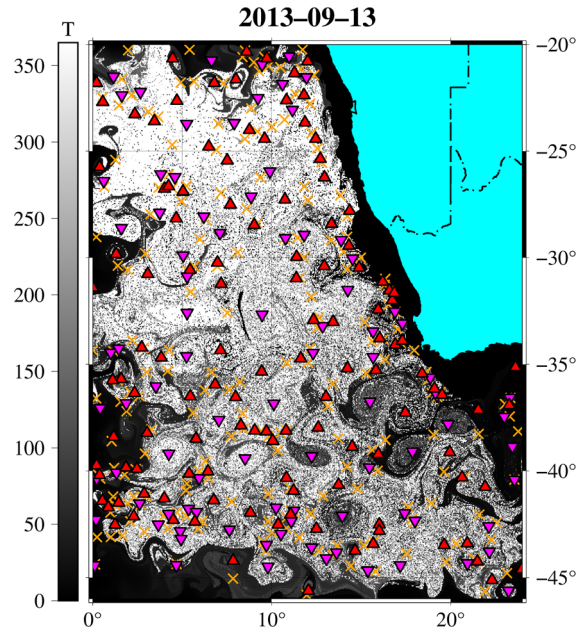

Figure 8
Particle 'age' map (Lagrangian T-map) on September 13, 2013, at a depth of 266 m. The color shows the time interval between the launch of particles on the specified date and the moment when one of the boundaries of the area is reached. In other words, the scale shows the time T of reaching the corresponding border of the region within a year ago from the date indicated on each frame/map. The white color paints the points that were within the borders of this region during the year from this date or were at the time of the launch of the markers on the shelf. The triangles and crosses are the same as in the previous figures

with other particles. At the same time other particles travel in the opposite direction westward overcoming a distance of more than 1100 km (Fig. 9). In the north direction, the distance travelled by the particles during a year exceeds 2200 km and 1100 km southward (Fig. 10). Thus, the dominant direction of the particles involved in water mixing is the northeast.

The φ-end-map (Fig. 11) complements the map with the zonal displacements (Fig. 9). The scale indicates the latitude at which the water particles crossed the prime meridian from west to east. Figure 11 also shows how far the water particles have spread in an easterly direction. It can be seen that the particles that crossed the 0° meridian propagate almost zonally. These particles travel a considerable distance to the east spreading almost to the eastern border of the basin in the latitude band 35–45° S. They do not cross the cores of eddies, by passing them along the periphery (see pls Fig. 12).

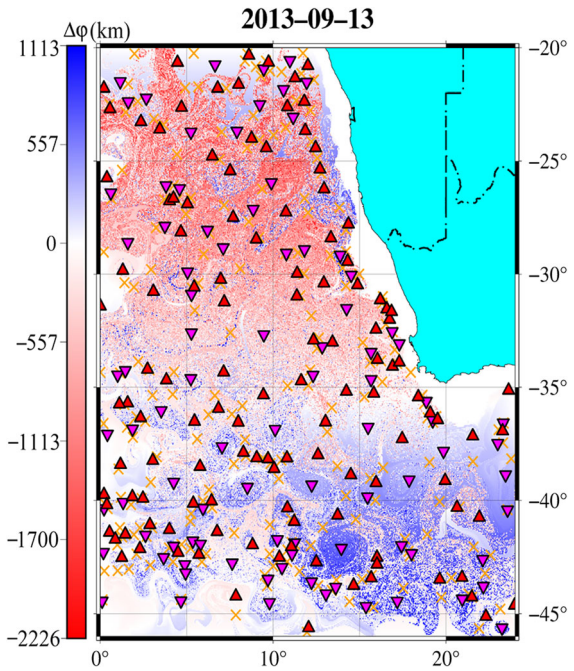

Figure 9
Zonal displacement of the particles on September 13, 2013, at a depth of 266 m. The scale indicates the zonal displacement (in km) which is the displacement of water particles eastward/ westward within 365 days from this date. The red color (negative values) highlights the waters that have shifted eastward, and the blue color (positive values) is for the waters shifted westward. The triangles and crosses are the same as in the previous figures

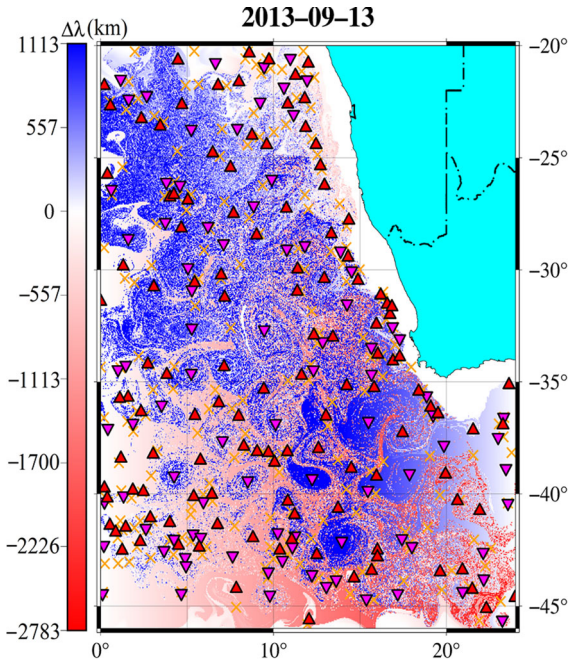

Figure 10
Meridional displacement of the particles on September 13, 2013, at a depth of 266 m. The scale indicates the meridional displacement (in km) which is the displacement of water particles northward/ southward within 365 days from this date. The red color (negative values) highlights the waters that have shifted northward, and the blue color (positive values) is for the waters shifted southward. The triangles and crosses are the same as in the previous figures

Thus, the analysis of Lagrangian maps (Figs. 6, 7, 8, 9, 10, 11, 12) shows that the eddies in the study region intensely interact with the surrounding waters. This means that the eddies formed as a result of the destruction of the Agulhas rings can change the structure of their waters while remaining in the Cape Basin. Here the waters of the Agulhas leakage mix with the waters of the South Atlantic Gyre and the Benguela Current, and the thermohaline properties of the Agulhas eddies change, as the warm and salty waters of the Indian Ocean mix with fresher and colder ones. The water particles of the South Atlantic Gyre cross the western border of the region and travel more than 500 km in an easterly direction, mixing with other particles. The Benguela Current appears in Figs. 6, 7, 8, 9, 10 as a line of eddies located along the coast of West Africa.

3.4. Thermohaline Analysis

Figure 12 presents the salinity field at a depth of 266 m. One can see in this figure a visual manifestation of the Agulhas leakage in the form of red spots with increased salinity values of water. The distribution of temperature in the water basin (not shown) is similar to the distribution of salinity. These red spots extend from the eastern border of the water basin to the northwest. The location of these red spots corresponds to the position of the eddies in Fig. 6. These eddies are formed from the rings of the Agulhas Current as a result of division into eddy structures of smaller scales. It can be seen that the waters of Agulhas leakage extend beyond the Walvis Ridge, actually to the northern part of the region. Benguela upwelling manifests itself in the coastal region. The upwelling process is accompanied by the formation of a significant number of mesoscale eddies both cyclones and anticyclones, along the

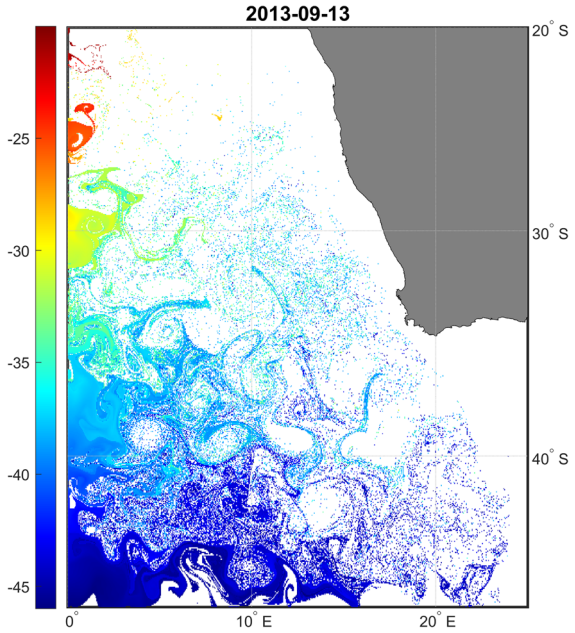

Figure 11
Map of determining the latitude where the particles crossed the prime meridian (Lagrangian φ-end-map) on September 13, 2013, at a depth of 266 m. The color shows the value of latitude where the points (particles) cross the 0° meridian within 365 days from this date

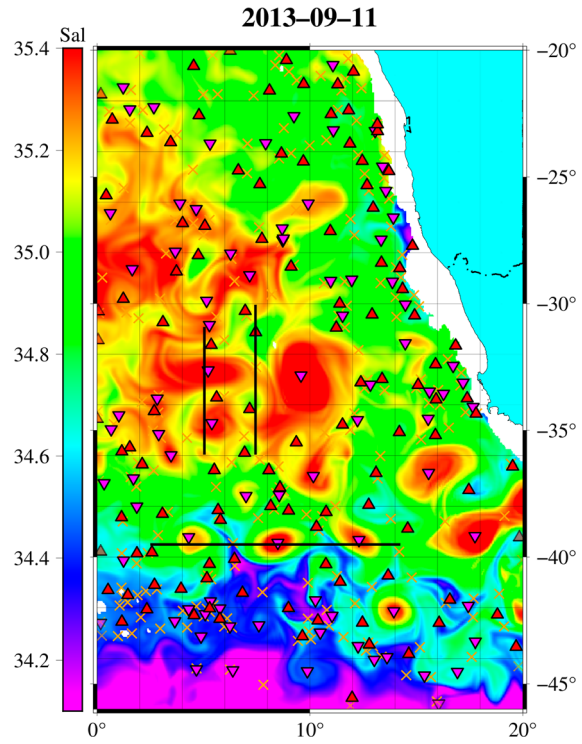

Figure 12
Salinity field on September 11, 2013, at a depth of 266 m. The cross-sections on which the vertical profiles of the eddies are indicated by black lines. The triangles and crosses are the same as in the previous figures

coastline boundary. It is important to emphasize that these eddies are stable locally and are observed on all maps throughout the period under consideration (see also Figure A7 Suppl. Mat.). However, the formation of eddies from the parent rings of the Agulhas Current occurs already in the Cape Basin (Fig. 4).

Then we analyzed the eddies indicated in the cross-sections (Fig. 12). The zonal section of 39.6°S passes through the centers of three AEs (Fig. 13). The meridional section of 5°E passes through the centers of two AEs (Fig. 14), and the meridional section of 7.5°E passes through the centers of two CEs (Fig. 15). Notice that these eddies are also manifested in Fig. 6 (S-map), Fig. 7 (O-map), and Fig. 8 (T-map). This once again emphasizes that the waters in the eddies differ from the surrounding waters both in origin and properties. Figure 7 reveals that both considered AE and CE consist mainly of particles that are colored green. They correspond to waters that arrived from the Indian Ocean and belong to the Agulhas leakage. Figures 13, 14, 15 show the vertical cross-sections of the temperature and salinity anomalies. The anomalies are estimated relative to the mean climatic fields based on the GLORYS12V1 data for 1993–2021. One can see that the temperature and salinity anomalies in the eddies reach ± 4 °C and ± 0.5–0.6 psu, respectively.

4. Discussion

We analyze the property of the water particles in the area where there is a mixing of waters originating from the Agulhas Current with the waters of the South Atlantic Gyre and the Benguela Current. These processes occur mainly in the Cape Basin where many mesoscale cyclones and anticyclones are generated. One can see in Fig. 1 that anticyclones have longer trajectories compared to cyclones. Anticyclones also have longer lifespans than cyclones. Moving to the west, anticyclones deviate to the equator, while cyclones deviate to the south. These

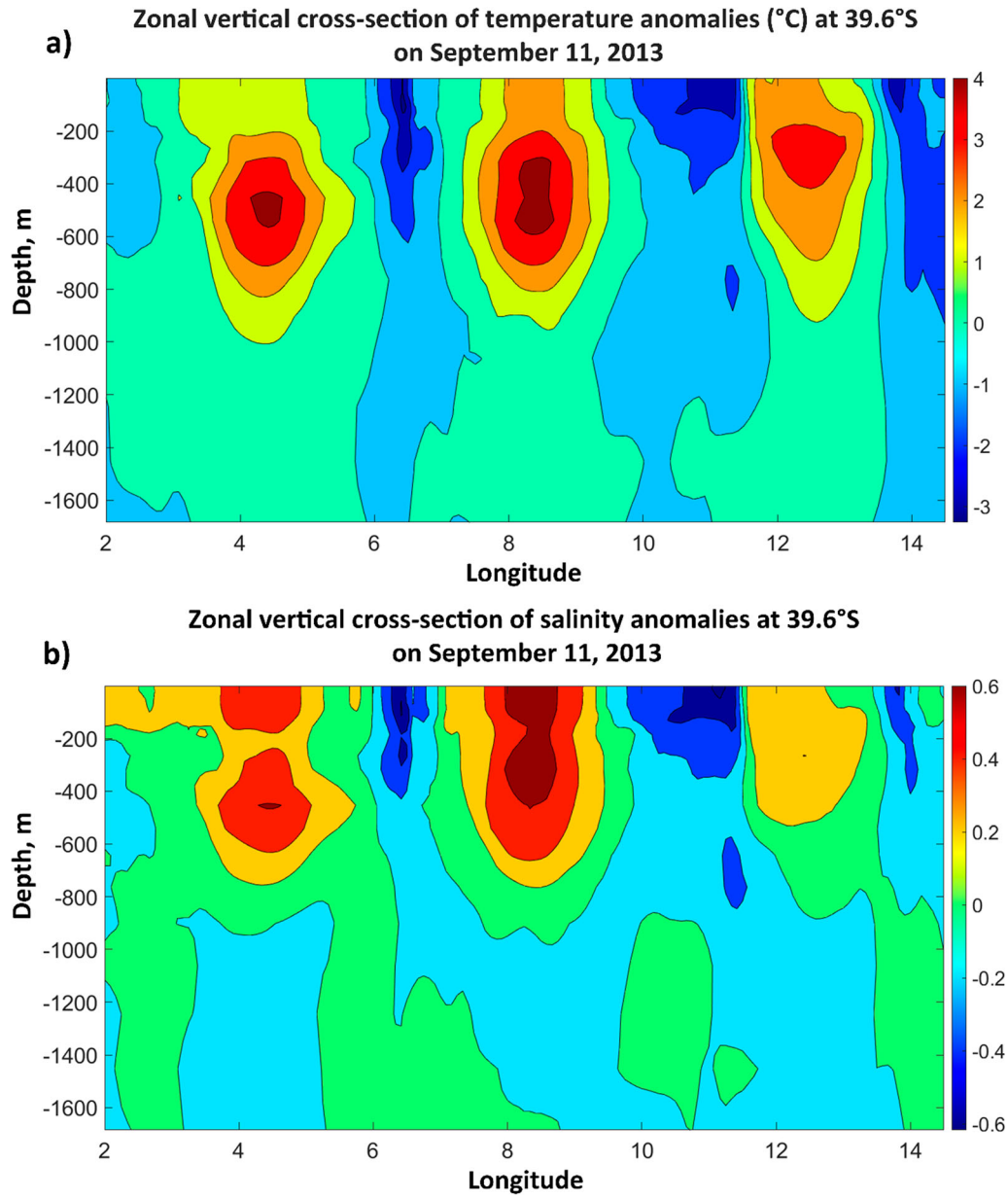

Figure 13
Zonal vertical cross-section of temperature (°C) and salinity anomalies for three AEs at 39.6°S on September 11, 2013

features of the Agulhas eddies were considered by Chelton et al. (2011) and discussed in detail by Gnevyshev et al. (2021).

One of the most interesting phenomena of the South Atlantic is the Agulhas leakage which is the link between the oceans; thus, the waters of the Indian Ocean are transported to the Atlantic. Estimates of the volume of the Agulhas leakage vary greatly. In this paper, we argue that the properties of the waters involved in the Agulhas leakage are significantly influenced by the waters of the South Atlantic Gyre and the Benguela Current. We emphasize that eddies generated near the coast are stable locally and are observed on all maps

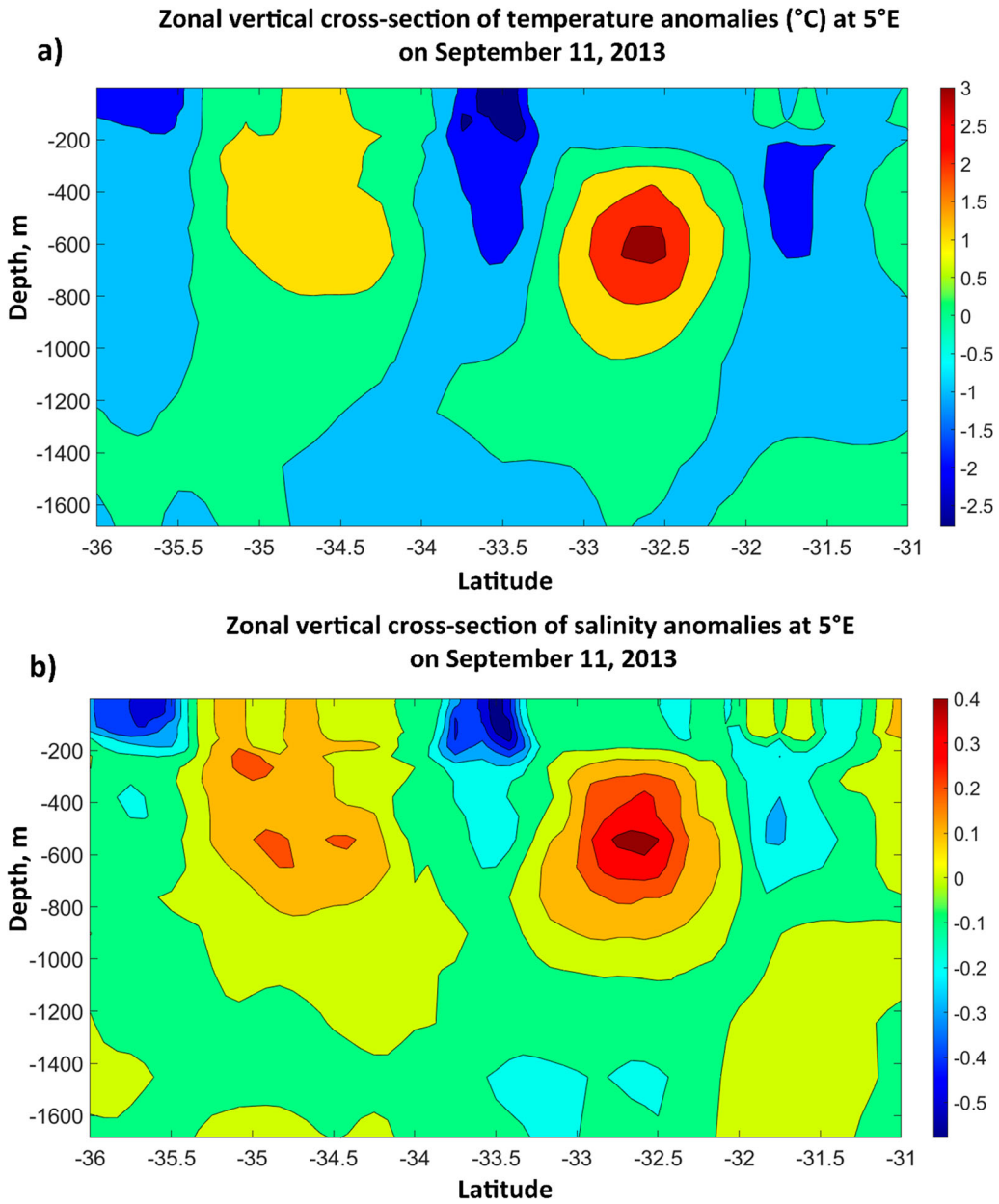

Figure 14
Meridional vertical cross-section of temperature (°C) and salinity anomalies for two AEs at 5°E on September 11, 2013

throughout the period under consideration (see also Figure A7 Suppl. Mat.).

We chose for the Lagrangian analysis a depth of 266 m to exclude the effect of Benguela upwelling and eddies generated in the upwelling. We were also based on the study by Guerra et al. (2022). See please Figs. 7, 10, and 13 in (Guerra et al., 2022). Figures 7, 10, and 13 show that 266 m is closer to the center of the eddy cores than 500 m. The chosen depth allows us to compare our results with the results of Guerra et al. (2022). Although our Figs. 13, 14, 15 show that the center of the eddy cores is located closer to 500 m, we left the depth of 266 m to have a

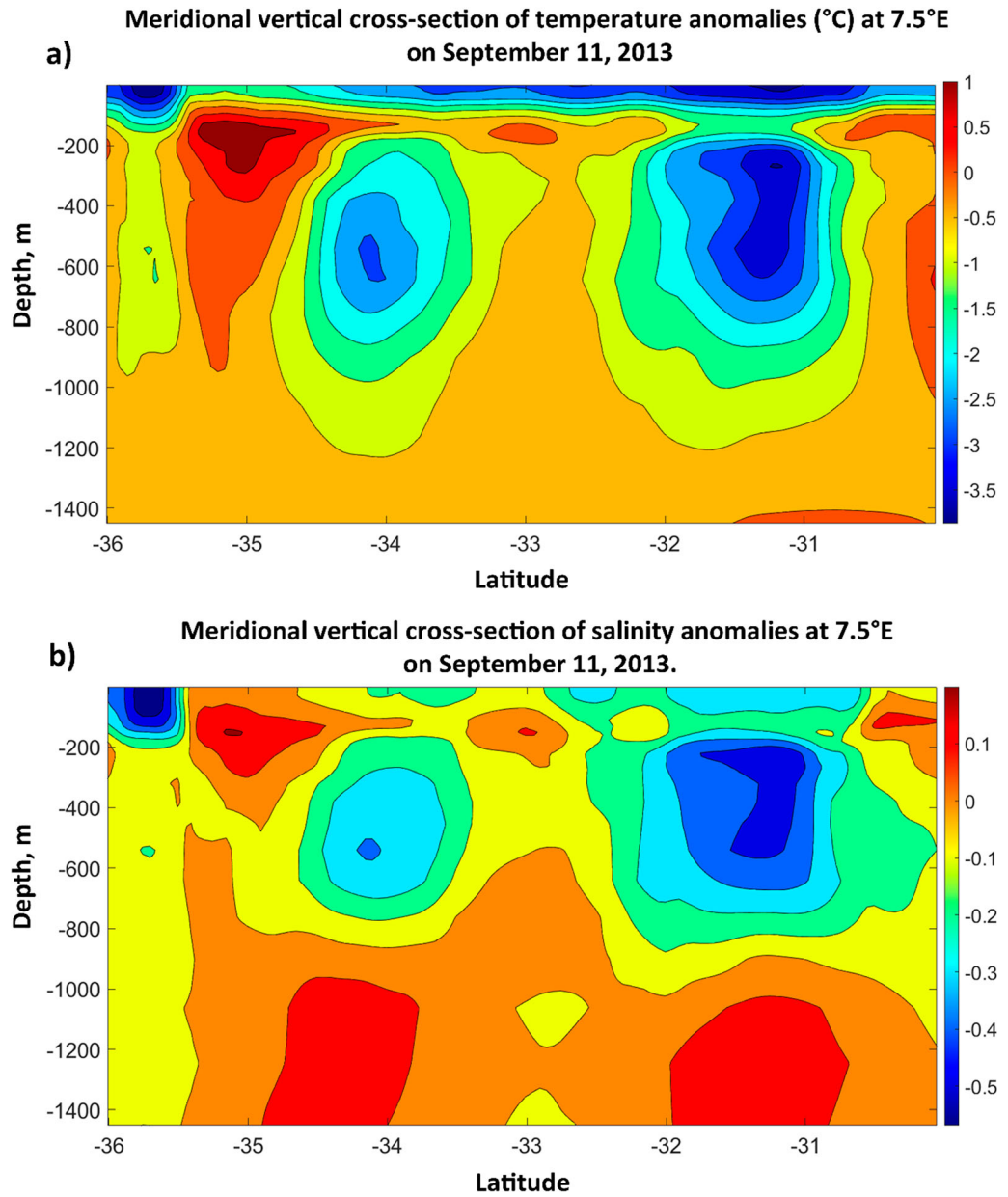

Figure 15
Meridional vertical cross-section of temperature (°C) and salinity anomalies for two CEs at 7.5°E on September 11, 2013

comparison with the results by Guerra et al. (2022) (see pls Figs. 10 and 13 by Guerra et al., 2022).

In this study, we examined the spread of particles of various origins in the Cape Basin and showed that the mixing process can be the result of the formation of water masses with different properties. This means that the mixing of the particles changes the structure of water masses in the region. Guerra et al. (2022) discussed two types of them with different properties: type I, temperature 16.2 ± 0.6 °C, salinity 35.6 ± 0.1, and type II, temperature 12.9 ± 0.7 °C, salinity 35.2 ± 0.1. Notice, that the thermohaline properties of water in eddies differ from the properties of the surrounding water. This is shown in the

article by Malysheva et al. (2020) using T/S diagrams. The two types of water masses discovered by Guerra et al. (2022) are obviously related to the different origins of the particles in the eddies they analyzed. Type I most likely corresponds to the waters of the Agulhas leakage, while type II can characterize the waters with the properties of the South Atlantic Gyre. However, we emphasize that this region is characterized by significant mixing of particles, as a result of which the eddy structures under consideration contain particles of various origins with different properties.

Thus, in the Cape Basin where the waters of the Agulhas Current mix with waters of the South Atlantic Gyre and the Benguela Current, the thermohaline properties of the Agulhas eddies change since the warm and salty waters of the Indian Ocean are mixed with fresher and colder. The mixing of the particles in the considered region is demonstrated using Lagrangian analysis (Figs. 6, 7, 8, 9, 10, 11). Zonal and meridional vertical cross-sections demonstrate different values of temperature and salinity in eddies located at the same latitude or longitude (Figs. 13, 14, 15). These properties can correspond to two types of water in the eddies mentioned by Guerra et al. (2022).

5. *Conclusion*

Using the eddy-resolving reanalysis GLORYS12V1 and the altimetric Mesoscale Eddy Trajectory Atlas product (META3.2), we estimate the properties of eddies in the region under consideration (20–46 °S, 0–20 °E) and find regional differences. Tracks of long-lived individual anticyclones and cyclones demonstrate mainly zonal eddy displacement. This means that the zonal components of the velocity dominate what can be explained by the influence of the β-effect. These eddies propagate almost rectilinearly. Under the influence of topography, especially when crossing the Walvis Ridge, tracks change the propagation azimuth, after which eddies propagate rectilinearly again. We also indicate the tendency of anticyclone tracks to shift to the equator and cyclones to the south.

The area under consideration is characterized by the high dynamic activity of mesoscale eddies. The main element of large-scale circulation is represented by the Agulhas leakage which is influenced by the South Atlantic Gyre, Benguela Current, and Benguela upwelling. The chosen depth of 266 m allows us not to take into account the influence of the Benguela upwelling on the eddy properties. Having applied the algorithm AMEDA we examine only long-lived eddies with a lifetime of > 60 days.

The novelty of this study lies in quantitative estimates of the characteristics of water mixing in the area under consideration. We have shown that the properties of the waters in the study area are determined by the influence of the Agulhas leakage, the South Atlantic Gyre, and the Benguela current. Lagrangian analysis shows that the main feature of the study area is the mixing of water particles of different origins. The waters of the South Atlantic Gyre interact significantly with the waters of Agulhas origin. This effect may impact the formation of the two-mode eddy structures explained in Guerra et al. (2022). Particles in the Agulhas leakage eddies originate not only from the Agulhas Current but also from the South Atlantic Gyre and the Benguela Current. Water particles spreading from the west and southwest travel hundreds of kilometers and fill the region. We have shown that the influence of the South Atlantic Gyre with particles moving to the east, is much more significant than previously thought. Water particles travel distances in an easterly direction exceeding 2700 km, while in the opposite direction (to the west) this distance is less than half.

Most eddies in the region have a radius of 40–50 km. We also estimate that the integral area for AEs is much bigger than the integral area for CEs despite the number of individual CEs with a lifetime of more than 60 days exceeding the number of long-lived AEs. The lifetime distribution of the eddies confirms that AEs are more long-lived than CEs. The majority of the eddies have a lifetime less than 100 days. However, some eddies with the longest path length have a lifetime more than 500 days. The mean orbital velocities vary mostly from 0.05 to 0.5 m/s for both AEs and CEs. Velocities of eddy drift have values of 3–13 km/day (3–15 cm/s) for both AEs and CEs. They are slightly higher for AEs

than CEs. We also show that the thermohaline anomalies of the eddy characteristics can reach ± 4 °C in temperature and ± 0.5–0.6 psu in salinity. This effect may impact the formation of the two-mode eddy structures explained in Guerra et al. (2022).

Acknowledgements

The work of T.B. and A.M. was supported by Russian Science Foundation, grant number 22-27-00004, and St Petersburg State University, grant number 94033410. The work of M.B. and A.U. on Lagrangian modelling and computing was supported by the POI FEBRAS Program (State Task No 121021700341-2).

Author Contributions TB and MB: conceived of the presented idea. MB and AU: developed the theory and performed the computations. TB and AM: verified the analytical methods. TB and MB: encouraged AM: and AU: to investigate a specific aspect and supervised the findings of this work. MB, AM, and AU: prepared figures. All authors discussed the results and contributed to the final manuscript.

Funding

This work was supported by Russian Science Foundation grant number 22-27-00004 St Petersburg State grant number 94033410, POI FEBRAS Program (State Task No 121021700341-2).

Data Availability

We used the GLORYS12V1 (Global Ocean Physics Reanalysis) data, a global ocean vortex-resolving reanalysis with a spatial resolution of 1/12 at 50 levels is available via the CMS (Copernicus Marine Service): https://datamarinecopernicuseuproductGLOBAL_MULTIYEAR_PHY_001_030/description.

Declarations

Conflict of Interest The authors declare that they have no known competing financial interests or personal relationships that could have appeared to influence the work reported in this paper.

References

Beismann, J.-O., Kase, R. H., & Lutjeharms, J. R. E. (1999). On the influence of submarine ridges on translation and stability of Agulhas rings. *Journal of Geophysical Research, 104*(C4), 7897–7906. https://doi.org/10.1029/1998JC900127

Belonenko, T., Zinchenko, V., Gordeeva, S., & Raj, R. P. (2020). Evaluation of heat and salt transports by mesoscale eddies in the Lofoten Basin. *Russian Journal of Earth Sciences, 20*, 6011. https://doi.org/10.2205/2020ES000720

Biastoch, A., Böning, C. W., & Lutjeharms, J. R. E. (2008). Agulhas leakage dynamics affects decadal variability in Atlantic overturning circulation. *Nature, 456*, 489–492. https://doi.org/10.1038/nature07426

Bryden, H. L., Beal, L. M., & Duncan, L. M. (2005). Structure and transport of the Agulhas Current and its temporal variability. *Journal of Oceanography, 61*, 479–492. https://doi.org/10.1007/s10872-005-0057-8

Budyansky, M. V., Prants, S. V., & Uleysky, MYu. (2022). Odyssey of Aleutian eddies. *Ocean Dynamics, 72*, 455–476. https://doi.org/10.1007/s10236-022-01508-w

Byrne, D. A., Gordon, A. L., & Haxby, W. F. (1995). Agulhas eddies: A synoptic view using geosat ERM data. *Journal of Physical Oceanography, 25*(5), 902–917. https://doi.org/10.1175/1520-0485(1995)025%3c0902:AEASVU%3e2.0.CO;2

Chelton, D. B., Schlax, M. G., & Samelson, R. M. (2011). Global observations of nonlinear mesoscale eddies. *Progress in Oceanography, 91*(2), 167–216. https://doi.org/10.1016/j.pocean.2011.01.002

Cheng, Yu., Putrasahan, D., Beal, L., & Kirtman, B. (2016). Quantifying Agulhas leakage in a high-resolution climate model. *Journal of Climate, 29*(19), 6881–6892. https://doi.org/10.1175/JCLI-D-15-0568.1

de Ruijter, W. P. M., Ridderinkhof, H., Lutjeharms, J. R. E., & Schouten, M. W. (2002). Direct observations of the flow in the Mozambique channel. *Geophysical Research Letters, 29*(10), 140-1–1403. https://doi.org/10.1029/2001GL013714

De Steur, L., Van Leeuwen, P. J., & Drijfhout, S. S. (2004). Tracer leakage from modeled Agulhas rings. *Journal of Physical Oceanography, 34*(6), 1387–1399. https://doi.org/10.1175/1520-0485(2004)034%3c1387:TLFMAR%3e2.0.CO;2

Doglioli, A. M., Blanke, B., Speich, S., & Lapeyre, G. (2007). Tracking coherent structures in a regional ocean model with wavelet analysis: Application to Cape Basin eddies. *Journal of*

Geophysical Research: Oceans. https://doi.org/10.1029/2006JC003952

Doglioli, A. M., Veneziani, M., Blanke, B., Speich, S., & Griffa, A. (2006). A Lagrangian analysis of the Indian-Atlantic interocean exchange in a regional model. *Geophysical Research Letters, 33*(14), 1–5. https://doi.org/10.1029/2006GL026498

Donners, J., Drijfhout, S. S., & Coward, A. C. (2004). Impact of cooling on the water mass exchange of Agulhas rings in a high resolution ocean model. *Geophysical Research Letters, 31*(16), L16312. https://doi.org/10.1029/2004GL020644

Drijfhout, S. S., & de Vries, P. (2003). Impact of eddy-induced transport on the Lagrangian structure of the upper branch of the thermohaline circulation. *Journal of Physical Oceanography, 33*(10), 2141–2155. https://doi.org/10.1175/1520-0485(2003)033%3c2141:IOETOT%3e2.0.CO;2

Duncombe Rae, C. M. (1991). Agulhas retroflection rings in the South Atlantic Ocean: An overview. *South African Journal of Marine Science, 11*(1), 327–344. https://doi.org/10.2989/025776191784287574

Duncombe Rae, C. M., Garzoli, S. L., & Gordon, A. L. (1996). The eddy field of the southeast Atlantic Ocean: A statistical census from the Benguela sources and transports project. *Journal of Geophysical Research, 101*(11), 949–964. https://doi.org/10.1029/95JC03360

Durgadoo, J. V., Ruhs, S., Biastoch, A., & Boning, C. W. B. (2017). Indian Ocean sources of Agulhas leakage. *Journal of Geophysical Research: Oceans, 122*, 3481–3499. https://doi.org/10.1002/2016JC012676

Garzoli, S. L., & Gordon, A. L. (1996). Origins and variability of the Benguela current. *Journal of Geophysical Research, 101*(C1), 897–906. https://doi.org/10.1029/95JC03221

Gnevyshev, V. G., Malysheva, A. A., Belonenko, T. V., & Koldunov, A. V. (2021). On Agulhas eddies and Rossby waves travelling by forcing effects. *Russian Journal of Earth Sciences, 21*, ES5003. https://doi.org/10.2205/2021ES000773

Goni, G. J., Garzoli, S. L., Roubicek, A. J., Olson, D. B., & Brown, O. B. (1997). Agulhas ring dynamics from TOPEX/POSEIDON satellite altimeter data. *Journal of Marine Research, 55*(5), 861–883. https://doi.org/10.1357/0022240973224175

Gordon, A. L. (1985). Indian-Atlantic transfer of thermocline water at the Agulhas retroflection. *Science, 227*(4690), 1030–1033. https://doi.org/10.1126/science.227.4690.1030

Gordon, A. L., & Haxby, W. F. (1990). Agulhas eddies invade the south Atlantic: Evidence from geosat altimeter and shipboard conductivity-temperature-depth survey. *Journal of Geophysical Research: Oceans, 5*(C3), 3117–3125. https://doi.org/10.1029/JC095iC03p03117

Gordon, A. L., Lutjeharms, J. R. E., & Grundlingh, M. L. (1987). Stratification and circulation at the Agulhas retroflection. *Deep Sea Research Part A, 34*, 565–599. https://doi.org/10.1016/0198-0149(87)90006-9

Gordon, A. L., Weiss, R. F., Smethie, W. M., Jr., & Warner, M. J. (1992a). Thermocline and intermediate water communication between the South Atlantic and Indian Oceans. *Journal of Geophysical Research: Oceans, 97*(C5), 7223–7240. https://doi.org/10.1029/92JC00485

Gordon, A. L., Weiss, R. F., Smethie, W. M., & Warner, M. J. (1992b). Thermocline and intermediate water communication between the South Atlantic and Indian Ocean. *Journal of Geophysical Research, 97*(C5), 7223–7240. https://doi.org/10.1029/92JC00485

Guerra, L. A. A., Mill, G. N., & Paiva, A. M. (2022). Observing the spread of Agulhas leakage into the Western South Atlantic by tracking mode waters within ocean rings. *Frontiers in Marine Science., 9*, 958733. https://doi.org/10.3389/fmars.2022.958733

Hutchings, L., van der Lingen, C. D., Shannon, L. J., Crawford, R. J. M., Verheye, H. M. S., Bartholomae, C. H., van der Plas, A. K., Louw, D., Kreiner, A., Ostrowski, M., Fidel, Q., Barlow, R. G., Lamont, T., Coetzee, J., Shillington, F., Veitch, J., Currie, J. C., & Monteiro, P. M. S. (2009). The Benguela Current: An ecosystem of four components. *Progress in Oceanography, 83*(1–4), 15–32. https://doi.org/10.1016/j.pocean.2009.07.046

Kamenkovich, V. M., Leonov, Y. P., Nechaev, D. A., Byrne, D. A., & Gordon, A. L. (1996). On the influence of bottom topography on the Agulhas eddy. *Journal of Physical Oceanography, 26*(6), 892–912. https://doi.org/10.1175/1520-0485(1996)026%3c0892:OTIOBT%3e2.0.CO;2

Le Vu, B., Stegner, A., & Arsouze, T. (2018). Angular Momentum Eddy Detection and Tracking Algorithm (AMEDA) and its application to coastal eddy formation. *Journal of Atmospheric and Oceanic Technology, 35*(4), 739–762. https://doi.org/10.1175/JTECH-D-17-0010.1

Lutjeharms, J. R. E., & Valentine, H. R. (1988). Evidence for persistent Agulhas rings southwest of Cape Town. *South African Journal of Science, 84*, 781–783.

Lutjeharms, J. R. E., & van Ballegooyen, R. C. (1988). The retroflection of the Agulhas Current. *Journal of Physical Oceanography, 18*, 1570–1583. https://doi.org/10.1175/1520-0485(1988)018%3c1570:TROTAC%3e2.0.CO;2

Malysheva, A. A., Belonenko, T. V., & Iakovleva, D. A. (2022). Characteristics of two eddies of different polarity in the Agulhas Current. *Journal of Hydrometeorology and Ecology., 68*, 478–493. https://doi.org/10.33933/2713-3001-2022-68-478-493. Gidrometeorologiya i Ekologiya In Russian.

Malysheva, A. A., Koldunov, A. V., Belonenko, T. V., & Sandalyuk, N. V. (2018). Vortices of Agulhas leakage inferred from altimeter data. *Uchenye Zapiski Rossijskogo Gosudarstvennogo Gidrometeorologicheskogo Universiteta [Scientific Notes of the Russian State Hydrometeorological University], 52*, 154–170. [In Russian].

Malysheva, A. A., Kubryakov, A. A., Koldunov, A. V., & Belonenko, T. V. (2020). Estimating Agulhas leakage by means of satellite altimetry and argo data. *Izvestiya, Atmospheric and Oceanic Physics, 56*, 1581–1589. https://doi.org/10.1134/S0001433820120476

Matano, R. P., & Beier, E. J. (2003). A kinematic analysis of the Indian/Atlantic inter-ocean exchange. *Deep-Sea Research II, 50*, 229–250.

Olson, D. B., & Evans, R. H. (1986a). Rings of the Agulhas current. *Deep Sea Research Part a: Oceanographic Research Papers, 33*(1), 27–42. https://doi.org/10.1016/0198-0149(86)90106-8

Olson, D., & Evans, R. (1986b). Rings of the Agulhas Current. *Deep-Sea Research, Part a: Oceanographic Research Papers, 33*(1), 27–42. https://doi.org/10.1016/0198-0149(86)90106-8

Pedlosky, J. (1987). *Geophysical fluid dynamics*. Springer.

Pegliasco, C., Busché, C., Faugère, Y. (2022). Mesoscale Eddy Trajectory Atlas META3.2 Delayed-Time all satellites: version META3.2 DT allsat. https://doi.org/10.24400/527896/A01-2022.005.210802

Prants, S. V., Budyansky, M. V., Lobanov, V. B., Sergeev, A. F., & Uleysky, M. Y. (2020). Observation and Lagrangian analysis of

quasistationary Kamchatka trench eddies. *Journal of Geophysical Research: Oceans, 125*(6), e2020JC016187. https://doi.org/10.1029/2020jc016187

Prants, S. V., Budyansky, M. V., & Uleysky, MYu. (2014). Identifying Lagrangian fronts with favourable fishery conditions. *Deep Sea Research Part i: Oceanographic Research Papers, 90*, 27–35. https://doi.org/10.1016/j.dsr.2014.04.012

Prants, S. V., Budyansky, M. V., & Uleysky, MYu. (2018). How eddies gain, retain, and release water: A case study of a Hokkaido anticyclone. *Geophysical Research Letters, 123*(3), 2081–2096. https://doi.org/10.1002/2017jc013610

Prants, S. V., Uleysky, MYu., & Budyansky, M. V. (2017). *Lagrangian oceanography: Large-scale transport and mixing in the ocean*. Springer-Verlag.

Reason, C. J. C., Lutjeharms, J. R. E., Hermes, J., Biastoch, A., & Roman, R. E. (2003). Inter-ocean fluxes south of Africa in an eddy permitting model. *Deep Sea Research Part II, 50*, 281–298. https://doi.org/10.1016/S0967-0645(02)00385-5

Richardson, P. L. (2007). Agulhas leakage into the Atlantic estimated with subsurface floats and surface drifters. *Deep-Sea Research Part I, 54*(8), 1361–1389. https://doi.org/10.1016/j.dsr.2007.04.010

Sandalyuk, N. V., & Belonenko, T. V. (2018). Mesoscale vortex dynamics in the Agulhas Current from satellite altimetry data. *Sovremennye Problemy Distantsionnogo Zondirovaniya Zemli iz Kosmosa Modern problems of remote sensing of the Earth from space., 15*(5), 179–190. https://doi.org/10.21046/2070-7401-2018-15-5-179-190. In Russian.

Sandalyuk, N. V., & Belonenko, T. V. (2021). Three-Dimensional Structure of the mesoscale eddies in the Agulhas Current region from hydrological and altimetry data. *Russian Journal of Earth Sciences, 21*, ES4005. https://doi.org/10.2205/2021ES000764

Schmid, C., Boebel, O., Zenk, W., Lutjeharms, J. R. E., Garzoli, S. L., Richardson, P. L., & Barron, C. (2003). Early evolution of an Agulhas Ring. *Deep Sea Research Part II: Topical Studies in Oceanography, 50*(1), 141–166. https://doi.org/10.1016/S0967-0645(02)00382-X

Schmitz, W. J. (1995). On the interbasin-scale thermohaline circulation. *Reviews of Geophysics, 33*(2), 151–173. https://doi.org/10.1029/95RG00879

Schouten, M. W., De Ruijter, W. P. M., Van Leeuwen, P. J., & Lutjeharms, J. R. E. (2000). Translation, decay and splitting of Agulhas rings in the southeastern Atlantic Ocean. *Journal of Geophysical Research: Oceans, 105*(C9), 21913–21925. https://doi.org/10.1029/1999JC000046

van Sebille, E., van Leeuwen, P. J., Biastoch, A., Barron, C. N., & de Ruijter, W. P. M. (2009). Lagrangian validation of numerical drifter trajectories using drifting buoys: Application to the Agulhas system. *Ocean Modelling, 29*, 269–276. https://doi.org/10.1016/j.ocemod.2009.05.005

Wang, Y., Olascoaga, M. J., & Beron-Vera, F. J. (2015). Coherent water transport across the South Atlantic. *Geophysical Research Letters, 42*(10), 4072–4079. https://doi.org/10.1002/2015gl064089

(Received January 21, 2023, revised July 11, 2023, accepted July 19, 2023)